International Journal of Innovative Computing, Information and Control
Volume **13**, Number **6**, December **2017**

ICIC International ©2017 ISSN 1349-4198
pp. **2067–2087**

TRACKING CONTROL VIA ROBUST DYNAMIC SURFACE CONTROL FOR HYPERSONIC VEHICLES WITH INPUT SATURATION AND MISMATCHED UNCERTAINTIES

Jingguang Sun, Shenmin Song* and Guanqun Wu

Center for Control Theory and Guidance Technology
Harbin Institute of Technology
No. 92, West Dazhi Street, Harbin 150001, P. R. China
{ sunjingguanghit; wgqwuguanqun }@163.com; *Corresponding author: songshenmin@hit.edu.cn

Received March 2017; revised July 2017

Abstract. *This thesis investigates the tracking control problem of hypersonic vehicles subject to mismatched uncertainties and input saturation. Firstly, the feedback linearization for longitudinal model of hypersonic vehicles is reasonably decomposed into two subsystems that include velocity and altitude subsystem. Secondly, for these two subsystems, an anti-saturation robust dynamic surface controller is designed using the auxiliary system and dynamic surface control (DSC) technique with compensating signals, respectively. The controllers can not only avoid the "explosion of complexity" in the backstepping design, but also remove the effect of the error caused by the first-order filter. Finally, Lyapunov theory is used to prove the stability of the designed controller strictly, and the numerical simulations of the longitudinal model of the hypersonic vehicles are carried out, which further demonstrate the robustness of the designed control scheme.*
Keywords: Hypersonic vehicles, Dynamic surface control, Tracking control, Input saturation, Mismatched uncertainty

1. **Introduction.** Hypersonic vehicles refer to the aircraft whose flight speed is greater than 5 Mach, which has fast speed, strong penetration ability, and therefore, it is of great military and economic value [1,2]. In comparison with traditional vehicles, the unique integrated design of hypersonic vehicles results in the high nonlinearity and strong coupling among its airframe, propulsion system and structural dynamics [3,4]. From the above, we can see that the hypersonic vehicles have large flight envelop and complicated flight environment. Its aerodynamic characteristics can change violently, and its model uncertainty is strong. Therefore, the robust controller is designed for the hypersonic vehicles in presence of unknown factors, which is one of the key technologies to ensure the safe and effective flight of the hypersonic vehicles [5].

In recent years, domestic and foreign experts and scholars majoring in the field of control have embarked on extensive researches and explorations. Foreign scholars have made extensive researches based on linear and nonlinear methods. The linear design methods are shown in [6,7]. It is well known that due to the complex nonlinear characteristics of hypersonic vehicles, the controller design method based on linear mode cannot meet the control performance requirements of the system. In [6,7], the designed controllers within a small scope around a certain equilibrium limits do not have good robustness. In order to obtain better control performance, the nonlinear control method was applied to the design of the hypersonic vehicles controller [8-12]. In [8], the hypersonic vehicles with parametric uncertainties were chosen as control object. A nonlinear controller was designed based on the dynamic inverse method and stochastic robust control method, which can obtain good tracking performance. Based on the feedback linearization method, a sliding mode

controller for hypersonic vehicles was designed in [9,10]. In [11], focused on hypersonic vehicle with TS disturbance modeling and disturbances, a robust tracking controller was designed using nonlinear disturbance observer. In [12], an anti-windup controller was proposed for air-breathing hypersonic vehicles, based on disturbance observer. However, it is more universal that mismatched disturbances (the disturbances are not in the input channel) occur in hypersonic vehicles. The mismatched disturbances that resulted from the dramatic changes in flight environments may influence the states directly, for example, which may be some mismatched uncertainties between the feedback linearization model and the nonlinear system model in [13,14]. For nonlinear systems with mismatched uncertainties, the back-stepping method is widely used in aerospace field. In [15], an adaptive back-stepping controller was designed for hypersonic vehicles, which can solve parameter uncertainty and fault of actuator. In [16], hypersonic flight vehicles with mismatched disturbances were analyzed using disturbance observer. An exponential sliding mode controller was designed for hypersonic vehicle subject to the mismatched uncertainties based on back-stepping method in [17]. In [18,19], an adaptive neural network back-stepping controller was designed for hypersonic vehicles subject to unmodeled dynamics and input saturation. For the back-stepping method, when the order of the control system is high, the explosion of complexity is easy to appear. In order to solve this problem, focusing on nonlinear systems, an adaptive dynamic surface controller back-stepping controller was designed using dynamic surface control technique and fuzzy control theory, which guarantees the closed-loop system signal bounded in [20]. In [21], focusing on nonlinear systems, a robust back-stepping controller was designed, which compensates the error of the virtual derivative by using the compensation signal of the command filter. In [22], concentrating on uncertain nonlinear systems, an adaptive dynamic surface controller was designed using command filter. Not only the "explosion of complexity" is avoided in the back-stepping, but also the effect of the errors is removed caused by command filter. In [23], based on the DSC and radial basis function neural network, an adaptive dynamic surface controller was designed for a class of nonlinear systems with unknown upper bound and all signals of the closed-loop system are bounded.

During the process of actual design of control system, if the input constraint is not considered, the problem of actuator saturation may emerge in the practical actuation, which will lead to the weakening of the system control performance, or even the system instability. In [24], based on the command filter technology, an adaptive anti-saturation tracking controller was designed for uncertain MIMO nonlinear systems with input constraints. In [25], focusing on a class of nonlinear systems with input constraints, the input saturation function was processed by mean value theorem and a neural network dynamic surface controller was proposed combining DSC and neural network control theory. For hypersonic vehicle with actuator dynamics and disturbances, a robust attitude controller with use of predictive sliding mode control and nonlinear disturbance observer, was proposed. For a hypersonic reentry vehicle subject to actuator saturation, a linear controller was designed based on a nonlinear extended state observer. In [27], a dynamic surface tracking controller was proposed to deal with hypersonic vehicle with aerodynamic parameter uncertainty and input constraint, by combining nonlinear disturbance observer and dynamic surface control in [28]. In [29,30], focusing on the hypersonic vehicles with input constraint and uncertain aerodynamic parameters, an adaptive dynamic surface robust controller was designed, which can achieve the stable tracking control of velocity and altitude. However, the introduction of neural network in some way augmented the complexity of the controller design, making it difficult to be applied in the engineering. In [31], for the hypersonic vehicles subject to input saturation problem, based on high-order differentiator, an adaptive neural network controller was designed, which can guarantee

that the closed-loop system is uniformly bounded. In [32], an adaptive robust controller was designed for the hypersonic vehicles with input saturation.

In order to further solve the anti-saturation tracking control problem of hypersonic vehicles, this paper designs an anti-saturation robust dynamic surface controller on the basis of the command filtering and the dynamic surface control, which can eliminate the impact of unmatched uncertainties, and can be able to control the input constraint at the same time. Compared with the literature listed above, this paper has innovative aspects as the following.

(1) Compared with [30], anti-saturation robust dynamic surface controller is designed using back-stepping method and command filter in the thesis, which adopts the robust compensation signals to eliminate the influence of mismatch.

(2) Compared with [29,32], the dynamic surface control technique is proposed with two kinds of first-order filters, which can remove the bounds of the derivative of the virtual control functions in this paper.

(3) Compared with [8-10], this paper takes input constraint into consideration, which makes the designed controllers have practical significance.

This paper is organized as follows. Firstly, the longitudinal input-output linearization model of hypersonic vehicles is established. Secondly, two anti-saturation robust dynamic surface back-stepping controllers are designed for velocity and altitude subsystem, respectively. Then, the corresponding stability of designed controller is analyzed by using the Lyapunov theory. Numerical simulations are given to verify the effectiveness of the designed tracking controllers in Section 4. In the end, the conclusion of the paper is presented.

Nomenclature

m – Mass, (kg)

S – Reference area, (m^2)

$\bar{c}$ – Mean aerodynamic chord, (m)

R_E – Earth radius, (m)

μ – Gravitational constant, (N m/kg^2)

h – Altitude, (m)

h_d – Reference command for altitude, (m)

V – Velocity, (m/s)

V_d – Reference command for velocity, (m/s)

ρ – Atmospheric density, (kg/m^3)

I_{yy} – Moment of inertia, (kg m^2)

L – Lift, (N)

D – Drag, (N)

T – Thrust, (N)

M – Pitching, (N m)

C_L – Lift, coefficient

C_L^{α} – First-order coefficient of α contribution to C_L

C_D – Drag coefficient

$C_D^{\alpha^i}$ – ith-order coefficient of α contribution to C_D

C_D^0 – Constant term in C_D

C_T – Thrust coefficient

β_0 and β_0' – Fuel-to-air ratio contribution to C_T^0

β_1 – Constant term in C_T^0

$C_{M,\alpha}$ – Contribution to moment due to angle of attack

$C_{M,\alpha}^{\alpha^i}$ – ith-order coefficient of α contribution to $C_{M,\alpha}$

$C_{M,\alpha}^0$ – Constant term in $C_{M,\alpha}$

C_{M,δ_e} – Contribution to moment due to elevator deflection

c_e – Elevator coefficient in C_{M,δ_e}

$C_{M,q}$ – Contribution to moment due to pitch rate

$C_{M,q}^{\alpha^i}$ – ith-order coefficient of α contribution to $C_{M,q}$

$C_{M,q}^0$ – Constant term in $C_{M,q}$

2. Preliminaries.

2.1. Hypersonic vehicles non-linear mode.

The rigid hypersonic vehicles model proposed by NASA Langley Research Center is below [10]

$$\begin{aligned}
\dot{V} &= \frac{T\cos\alpha - D}{m} - \frac{\mu}{r^2}\sin(\theta-\alpha)\\
\dot{h} &= V\sin(\theta-\alpha)\\
\dot{\alpha} &= -\frac{L+T\sin\alpha}{mV} + q + \left(\frac{g}{V} - \frac{V}{r}\right)\cos(\theta-\alpha)\\
\dot{\theta} &= q\\
\dot{q} &= \frac{M}{I_{yy}}
\end{aligned} \tag{1}$$

where

$$\begin{aligned}
&L = 0.5\rho V^2 S C_L\\
&D = 0.5\rho V^2 S C_D\\
&T = 0.5\rho V^2 S C_T\\
&M = 0.5\rho V^2 S\bar{c} C_M\\
&r = h + R_E\\
&C_L = C_L^{\alpha}\alpha\\
&C_D = C_D^{\alpha^2}\alpha^2 + C_D^{\alpha}\alpha + C_D^0\\
&C_T = C_T^0(\phi) = \begin{cases} \beta_0\phi & \text{if } \phi < 1\\ \beta_1 + \beta_0'\phi & \text{if } \phi > 1 \end{cases}\\
&C_M = C_M(\alpha) + C_M(\delta_e) + C_M(q)\\
&C_{M,\alpha}(\alpha) = C_{M,\alpha}^{\alpha^2}\alpha^2 + C_{M,\alpha}^{\alpha}\alpha + C_{M,\alpha}^0\\
&C_{M,\delta_e}(\delta_e) = c_e(\delta_e - \alpha)\\
&C_{M,q}(q) = (c/2V)\,q\left(C_{M,q}^{\alpha^2}\alpha^2 + C_{M,q}^{\alpha}\alpha + C_{M,q}^0\right)
\end{aligned}$$

V, h, and q are velocity, altitude, angle of attack, pitch angle, pitch rate of the hypersonic aircrafts, T, D, L, M, δ_e and ϕ mean thrust, drag, lift, pitching moment, the elevator deflection angle, the throttle setting, respectively. m, ρ, I_{yy}, S, and R_E denote mass of hypersonic vehicles, density of air, moment of inertia, gravitational constant, radius of the earth, $\bar{c}$ and c_e are constants. Other related variables and parameters in this model are listed in the nomenclature.

The second-order dynamical model of the engine can be described as

$$\ddot{\phi} = -2\zeta\omega_n\dot{\phi} - \omega_n^2\phi + \omega_n^2\phi_c \tag{2}$$

where ϕ is the throttle setting, ϕ_c is the demand of the control input, ω_n is the undamped natural frequency of the engine dynamics, and ζ is the damping ratio.

2.2. Input-output linearization model.

In order to facilitate the design of hypersonic vehicles control system and controller, the linearization system model is as follows [10].

$$\begin{aligned}
V^{(3)} &= f_V + b_{11}\phi_c + b_{12}\delta_e + \Delta f_V + \Delta b_{11}\phi_c + \Delta b_{12}\delta_e\\
h^{(4)} &= f_h + b_{21}\phi_c + b_{22}\delta_e + \Delta f_h + \Delta b_{21}\phi_c + \Delta b_{22}\delta_e
\end{aligned} \tag{3}$$

where ϕ_c and δ_e are control inputs, Δf_V, Δf_h, Δb_{11}, Δb_{12}, Δb_{21}, Δb_{22} are bounded items created by parameter uncertainly and external disturbance, and the definitions of f_V, f_h, b_{11}, b_{12}, b_{21} and b_{22} can be seen in [10].

Let

$$\begin{cases} \Delta x_{V3} = \Delta f_V + \Delta b_{11}\delta_e + \Delta b_{12}\phi_c \\ \Delta x_{h4} = \Delta f_h + \Delta b_{21}\delta_e + \Delta b_{22}\phi_c \\ u_V = b_{11}\phi_c + b_{12}\delta_z \\ u_h = b_{21}\phi_c + b_{22}\delta_z \\ \boldsymbol{x_V} = \begin{bmatrix} x_{V1} & x_{V2} & x_{V3} \end{bmatrix}^T = \begin{bmatrix} V & \dot{V} & \ddot{V} \end{bmatrix}^T \\ \boldsymbol{x_h} = \begin{bmatrix} x_{h1} & x_{h2} & x_{h3} & x_{h4} \end{bmatrix}^T = \begin{bmatrix} h & \dot{h} & \ddot{h} & \dddot{h} \end{bmatrix}^T \end{cases} \tag{4}$$

By applying (4), the system model (3) can be transformed into velocity and altitude subsystem which have triangular form with mismatched uncertainties

$$\begin{cases} \dot{x}_{V1} = x_{V2} + \Delta x_{V1} \\ \dot{x}_{V2} = x_{V3} + \Delta x_{V2} \\ \dot{x}_{V3} = f_V + u_V + \Delta x_{V3} \end{cases} \tag{5}$$

$$\begin{cases} \dot{x}_{h1} = x_{h2} + \Delta x_{h1} \\ \dot{x}_{h2} = x_{h3} + \Delta x_{h2} \\ \dot{x}_{h3} = x_{h4} + \Delta x_{h3} \\ \dot{x}_{V3} = f_h + u_h + \Delta x_{h4} \end{cases} \tag{6}$$

where Δx_{V1}, Δx_{V2}, Δx_{V3}, Δx_{h1}, Δx_{h2}, Δx_{h3} and Δx_{h4} are lumped mismatched uncertainties.

Consider the following forms of input saturation

$$u_i = \begin{cases} u_{i\max}, & u_{ic} \geq u_{i\max} \\ u_{ic}, & u_{i\min} < u_{ic} < u_{i\max} \\ u_{i\min}, & u_{ic} \leq u_{i\min} \end{cases} \quad (i = V, h) \tag{7}$$

where u_i is desired control input, $u_{i\min}$ is the minimum values of u_i, $u_{i\max}$ is the maximum values of u_i.

Control object: In the thesis, two anti-saturation robust dynamic surface controllers are designed for the system mode (5)-(7), so that the velocity V and the altitude h could track the reference signals V_d and h_d in finite-time subject to mismatched uncertainties and input saturation, respectively. Meanwhile, angle of attack α, pitch angle θ and pitch rate q are kept within a certain range.

2.3. **Related lemmas and assumptions.** To facilitate the control system design in this subsection, the following assumption is introduced firstly.

Lemma 2.1. [21]: *The compensating signals ξ_i for $i = 2, \ldots, n$ are defined as*

$$\begin{aligned} \dot{\xi}_1 &= -c_1\xi_1 - \xi_1 + \xi_2 + (x_{2,c} - a_1) \\ \dot{\xi}_i &= -c_i\xi_i - \xi_{i-1} + \xi_{i+1} + (x_{i+1,c} - a_i) \\ \dot{\xi}_n &= -c_n\xi_n - \xi_{n-1} \end{aligned} \tag{8}$$

where a_i and $x_{i+1,c}$ are first-order filter input and output. We can get that $\|\xi_i\|$ is bounded.

Assumption 2.1. *The disturbance Δx_{Vi} $(i = 1, 2, 3)$ is the unknown bounded uncertainty that has bounded derivative. That is to say, there is a positive constant $\tilde{\sigma}_{Vi}$ $(i = 1, 2, 3)$ satisfying the inequality as the following*

$$\Delta x_{Vi} \leq \tilde{\sigma}_{Vi} \quad (i = 1, 2, 3) \tag{9}$$

Assumption 2.2. *The disturbance* Δx_{hj} $(j = 1, 2, 3, 4)$ *is the unknown bounded uncertainty that has bounded derivative. That is to say, there is a positive constant* $\tilde{\sigma}_{hj}$ $(j = 1, 2, 3, 4)$ *satisfying the inequality as the following*

$$\Delta x_{hj} \leq \tilde{\sigma}_{hj} \quad (j = 1, 2, 3, 4) \tag{10}$$

3. **Main Results.** A robust DSC back-stepping control scheme is design to cope with mismatched uncertainties and input saturation of the system, which uses dynamic surface control with signal compensation and auxiliary system. The proposed approach not only avoids the "explosion of complexity" in the back-stepping method, but also removes the effect of the error caused by the first-order filter, which guarantees the fast convergence of tracking error and the system robustness for uncertainties.

3.1. **Robust DSC back-stepping controller design for velocity subsystem.** For system (5), an anti-saturation robust dynamic surface controller is designed. The specific process is as follows.

Step 1: Define the tracking error variable z_{V1} as

$$z_{V1} = x_{V1} - x_{Vd} \tag{11}$$

where x_{Vd} is reference velocity.

Computing the first order derivative of (11), we obtain

$$\dot{z}_{V1} = \dot{x}_{V1} - \dot{x}_{Vd} = x_{V2} - \dot{x}_{Vd} + \Delta x_{V1} \tag{12}$$

Define the virtual control functions x_{V2} as

$$\bar{x}_{V2} = -k_{V1} z_{V1} + \dot{x}_{Vd} + \omega_{V1} \tag{13}$$

where $k_{V1} > 0$ is a positive constant. The virtual controller (13) consists of two parts. (1) The nominal intermediate input $-k_{V1} x_{V1} + \dot{x}_{Vd}$. (2) ω_{V1} is the robust compensation input, which can eliminate the effect of uncertainties.

Substituting (13) into (12) yields

$$\dot{z}_{V1} = -k_{V1} z_{V1} + \omega_{V1} + \Delta x_{V1} \tag{14}$$

The compensation signal ω_{V1} is constructed by a low-pass filter

$$\omega_{V1} = -F_{V1}(s) \Delta x_{V1} \tag{15}$$

where $F_{V1}(s) = \lambda_{V1}/s + \lambda_{V1}$ is a low-pass filter.

When the bandwidth λ_{V1} of the filter is chosen large enough, the signal ω_{V1} approximately equals Δx_{V1}, which can eliminate the effects of mismatched uncertainties.

We define x_{V2d} satisfying as

$$\tau_{V2} \dot{x}_{V2d} + x_{V2d} = \bar{x}_{V2}, \; x_{V2d}(0) = \bar{x}_{V2}(0) \tag{16}$$

where x_{V2d} and $\bar{x}_{V2}$ are first-order filter input and output respectively, τ_{V2} is a positive constant.

To eliminate the effect of the error $x_{V2d} - \bar{x}_{V2}$, the compensating signal is defined as

$$\dot{\xi}_{V1} = -k_{V1} \xi_{V1} + \xi_{V2} + (x_{V2d} - \bar{x}_{V2}) \tag{17}$$

The compensated tracking error signal $\nu_{V1} = z_{V1} - \xi_{V1}$ and the compensation error signal $\rho_{V1} = \omega_{V1} + \Delta x_{V1}$.

Consider Lyapunov function as

$$V_{V1} = \frac{1}{2} \nu_{V1}^2 + \frac{1}{2} \rho_{V1}^2 \tag{18}$$

The time derivative of V_{V1} is given as

$$\begin{aligned}\dot{V}_1 &= \nu_{V1}\dot{\nu}_{V1} + \rho_{V1}\dot{\rho}_{V1} \\ &= \nu_{V1}\left(-k_{V1}z_{V1} + \omega_{V1} + \Delta x_{V1} + z_{V2} + x_{V2d} - \bar{x}_{V2} + k_{V1}\xi_{V1}\right. \\ &\quad \left.-\xi_{V2} - x_{V2d} + \bar{x}_{V2}\right) + \rho_{V1}\dot{\rho}_{V1} \\ &= \nu_{V1}\left(-k_{V1}z_{V1} + \rho_{V1} + z_{V2} + k_{V1}\xi_{V1} - \xi_{V2}\right) + \rho_{V1}\left(-\lambda_{V1}\rho_{V1} + \dot{\Delta}x_{V1}\right) \\ &= -k_{V1}\nu_{V1}^2 + \nu_{V1}\left(z_{V2} - \xi_{V2}\right) + \nu_{V1}\rho_{V1} - \lambda_{V1}\rho_{V1}^2 + \dot{\Delta}x_{V1}\rho_{V1}\end{aligned} \tag{19}$$

By using Young's inequality

$$\nu_{V1}\rho_{V1} \le \frac{1}{2}v_{V1}^2 + \frac{1}{2}\rho_{V1}^2, \quad \dot{\Delta}x_{V1}\rho_{V1} \le \frac{1}{2}\dot{\Delta}_{V1}^2 + \frac{1}{2}\rho_{V1}^2 \tag{20}$$

Substituting (20) into (19) yields

$$\begin{aligned}\dot{V}_1 &= -k_{V1}\nu_{V1}^2 + \nu_{V1}\left(z_{V2} - \xi_{V2}\right) + \frac{1}{2}v_{V1}^2 + \frac{1}{2}\rho_{V1}^2 - \lambda_{V1}\rho_{V1}^2 + \frac{1}{2}\dot{\Delta}_{V1}^2 + \frac{1}{2}\rho_{V1}^2 \\ &= -\left(k_{V1} - \frac{1}{2}\right)\nu_{V1}^2 + \nu_{V1}\left(z_{V2} - \xi_{V2}\right) - \left(\lambda_{V1} - 1\right)\rho_{V1}^2 + \frac{1}{2}\tilde{\delta}_{V1}^2\end{aligned} \tag{21}$$

Step 2: Define the tracking error variable

$$z_{V2} = x_{V2} - x_{V2d} \tag{22}$$

The time derivative of (22) can be written as

$$\dot{z}_{V2} = \dot{x}_{V2} - \dot{x}_{V2d} = x_{V3} + \Delta x_{V2} - \dot{x}_{V2d} \tag{23}$$

Define the virtual control functions $\bar{x}_{V3}$ as

$$\bar{x}_{V3} = -k_{V2}z_{V2} - z_{V1} + \dot{x}_{V2d} + \omega_{V2} \tag{24}$$

where $k_{V2} > 0$ is a positive constant.

The compensation signal ω_{V2} is constructed by a low-pass filter

$$\omega_{V2} = -F_{V2}(s)\Delta x_{V2} \tag{25}$$

where $F_{V2}(s) = \lambda_{V2}/s + \lambda_{V2}$ is a low-pass filter.

When the bandwidth λ_{V2} of filter is chosen large enough, the signal ω_{V2} approximately equals Δx_{V2}, which can eliminate the effects of mismatched uncertainties.

x_{V3d} is defined as

$$\tau_{V3}\dot{x}_{V3d} + x_{V3d} = \bar{x}_{V3},\ x_{V3d}(0) = \bar{x}_{V3}(0) \tag{26}$$

where x_{V3d} and $\bar{x}_{V3}$ are the input and output of the first-order filter, respectively, τ_{V3} is a positive constant.

To eliminate the effect of the error $x_{V3d} - \bar{x}_{V3}$, the compensating signals are defined as

$$\dot{\xi}_{V2} = -k_{V2}\xi_{V2} - \xi_{V1} + \xi_{V3} + \left(x_{V3d} - \bar{x}_{V3}\right) \tag{27}$$

We define the compensated tracking error signal $\nu_{V2} = z_{V2} - \xi_{V2}$ and the compensation error signal $\rho_{V2} = \omega_{V2} + \Delta x_{V2}$.

Choose the Lyapunov function as

$$V_{V2} = V_{V1} + \frac{1}{2}\nu_{V2}^2 + \frac{1}{2}\rho_{V2}^2 \tag{28}$$

Computing the first order derivative of V_{V2} yields

$$\begin{aligned}\dot{V}_2 &= \dot{V}_1 + \nu_{V2}\dot{\nu}_{V2} + \rho_{V2}\dot{\rho}_{V2} \\ &= \dot{V}_1 + \nu_{V2}\left(z_{V3} - k_{V2}z_{V2} - z_{V1} + k_{V2}\xi_{V2} + \xi_{V1} - \xi_{V3} + \rho_{V2}\right) + \rho_{V2}\dot{\rho}_{V2} \\ &= -\left(k_{V1} - \frac{1}{2}\right)\nu_{V1}^2 - \left(\lambda_{V1} - 1\right)\rho_{V1}^2 + \nu_{V1}\nu_{V2} \\ &\quad + \nu_{V2}\left(-k_{V2}\nu_{V2} + z_{V3} - \xi_{V3} + \rho_{V2} - \nu_{V1}\right) - \lambda_{V2}\rho_{V2}^2 + \dot{\Delta}_{V2}\rho_{V2} + \frac{1}{2}\tilde{\delta}_{V1}^2 \\ &= -\left(k_{V1} - \frac{1}{2}\right)\nu_{V1}^2 - \left(\lambda_{V1} - 1\right)\rho_{V1}^2 + \nu_{V2}\left(-k_{V2}\nu_{V2} + z_{V3} - \xi_{V3}\right) - \lambda_{V2}\rho_{V2}^2 \\ &\quad + \nu_{V2}\rho_{V2} + \dot{\Delta}_{V2}\rho_{V2} + \frac{1}{2}\tilde{\delta}_{V1}^2\end{aligned} \tag{29}$$

By using Young's inequality

$$\nu_{V2}\rho_{V2} \le \frac{1}{2}v_{V2}^2 + \frac{1}{2}\rho_{V2}^2, \quad \dot{\Delta}_{V2}\rho_{V2} \le \frac{1}{2}\dot{\Delta}_{V2}^2 + \frac{1}{2}\rho_{V2}^2 \tag{30}$$

Substituting (30) into (29), we have

$$\begin{aligned}\dot{V}_{V2} &\le -\left(k_{V1} - \frac{1}{2}\right)\nu_{V1}^2 - \left(\lambda_{V1} - 1\right)\rho_{V1}^2 - \left(k_{V2} - \frac{1}{2}\right)\nu_{V2}^2 - \left(\lambda_{V2} - 1\right)\rho_{V2}^2 \\ &\quad + \nu_{V2}\left(z_{V3} - \xi_{V3}\right) + \frac{1}{2}\tilde{\delta}_{V1}^2 + \frac{1}{2}\tilde{\delta}_{V2}^2 \\ &\le -\sum_{i=1}^{2}\left(k_{Vi} - \frac{1}{2}\right)k_{Vi}\nu_{Vi}^2 - \sum_{i=1}^{2}\left(\lambda_{Vi} - 1\right)\rho_{Vi}^2 \\ &\quad + \nu_{V2}\left(z_{V3} - \xi_{V3}\right) + \frac{1}{2}\tilde{\delta}_{V1}^2 + \frac{1}{2}\tilde{\delta}_{V2}^2\end{aligned} \tag{31}$$

Step 3: Define the tracking error variable

$$z_{V3} = x_{V3} - x_{V3d} \tag{32}$$

Computing the first order derivative of z_{V3}, we obtain

$$\dot{z}_{V3} = f_V + u_V + \Delta x_{V3} - \dot{x}_{V3d} \tag{33}$$

To handle input saturation, the auxiliary system (34) is introduced

$$\dot{\eta}_V = \begin{cases} -k_{V\eta}\eta_V - \dfrac{1}{\|\eta_V\|^2}\left(|\nu_{V3}\Delta u_V| + 0.5\Delta u_V^2\right)\eta_V - \Delta u_V - k_{V\gamma}\mathrm{sig}^{\gamma}\left(\nu_{V3}\right), & \|\eta_V\| \ge \sigma_V \\ 0 & \|\eta_V\| < \sigma_V \end{cases} \tag{34}$$

where $\mathrm{sig}^{\gamma}\left(\nu_{V3}\right) = |\nu_{V3}|^{\gamma}\,\mathrm{sign}\left(\nu_{V3}\right)$. $k_{V\eta}$, $k_{V\gamma}$ and γ are positive parameters and η_V is the state variable of the auxiliary system. σ_V is positive constant, $\Delta u_V = u_V - u_{Vc}$.

Remark 3.1. *From the hypersonic vehicles background, it can be seen that the input saturation may be symmetrical or asymmetric. The auxiliary system (34) can handle symmetrical and asymmetric input saturation.*

The compensated tracking error signal $\nu_{V3} = z_{V3} - \xi_{V3}$, and compensation error signal $\rho_{V3} = \omega_{V3} + \Delta x_{V3}$.

The compensating signal ξ_{V3} is defined as

$$\dot{\xi}_{V3} = -k_{V3}\xi_{V3} - \xi_{V2} \tag{35}$$

where k_{V3} is a positive constant.

The control law u_{Vc} is defined as

$$u_{Vc} = -k_{V3}z_{V3} - f_V - z_{V2} + \dot{x}_{V3d} + \omega_{V3} + k_{V4}\eta_V - \frac{v_{V3}\mu_V\left(v_{V3}\right)}{\psi_V^2 + \left\|v_{V3}\right\|^2} \tag{36}$$

$$\dot{\psi}_V = \begin{cases} -k_{V\psi}\psi_V - \dfrac{\mu_V\left(v_{V3}\right)\psi_V}{\psi_V^2 + \left\|v_{V3}\right\|^2}, & \left\|v_{V3}\right\| \geq \psi_\nu \\ 0, & \left\|v_{V3}\right\| < \psi_\nu \end{cases} \tag{37}$$

where $\mu_V\left(v_{V3}\right) = 0.5k_{V4}^2 v_{V3}^2$. k_{V3}, k_{V4}, $k_{V\psi}$ and ψ_ν are positive constants.

The compensation signal ω_{V3} is constructed by a low-pass filter

$$\omega_{V3} = -F_{V3}(s)\Delta x_{V3} \tag{38}$$

where $F_{V3}(s) = \lambda_{V3}/s + \lambda_{V3}$ is a low-pass filter.

Theorem 3.1. *Considering system (5) with Assumption 2.1, the state of closed-loop system is regulated under the anti-saturation robust dynamic surface controllers (34)-(37). The following conclusions can be obtained.*

(i) The variable v_{Vi} $(i = 1, 2, 3)$, ρ_{Vi} $(i = 1, 2, 3)$, η_V and ψ_V are uniformly ultimately bounded respectively;

(ii) The velocity tracking error converges to any small neighborhood.

Proof: Choose Lyapunov function as

$$V_{V3} = V_{V2} + \frac{1}{2}\nu_{V3}^2 + \frac{1}{2}\rho_{V3}^2 + \frac{1}{2}\eta_V^2 + \frac{1}{2}\psi_V^2 \tag{39}$$

Computing the derivative of V_{V3}, we have

$$\dot{V}_{V3} = \dot{V}_{V2} + \nu_{V3}\dot{\nu}_{V3} + \rho_{V3}\dot{\rho}_{V3} + \eta_V\dot{\eta}_V + \psi_V\dot{\psi}_V \tag{40}$$

According to (34)-(37), we can obtain

$$\begin{aligned} \dot{V}_{V3} = & \dot{V}_{V2} + \nu_{V3}\left(\omega_{V3} + \Delta x_{V3} - k_{V3}z_{V3} - z_{V2} - \dot{\xi}_{V3}\right) + k_{V4}\nu_{V3}\eta_V \\ & + \nu_{V3}\Delta u_V + \rho_{V3}\dot{\rho}_{V3} + \eta_V\dot{\eta}_V + \psi_V\dot{\psi}_V - \frac{v_{V3}^2\mu_V\left(v_{V3}\right)}{\psi_V^2 + \left\|v_{V3}\right\|^2} \\ = & -\sum_{i=1}^{2}\left(k_{Vi} - \frac{1}{2}\right)\nu_{Vi}^2 - \sum_{i=1}^{2}\left(\lambda_{Vi} - 1\right)\rho_{Vi}^2 + \frac{1}{2}\tilde{\delta}_{V1}^2 + \frac{1}{2}\tilde{\delta}_{V2}^2 \\ & + \nu_{V3}\left(-k_{V3}z_{V3} + k_{V3}\xi_{V3} + \rho_{V3}\right) + \rho_{V3}\dot{\rho}_{V3} + k_{V4}\nu_{V3}\eta_V \\ & + \nu_{V3}\Delta u_V + \eta_V\dot{\eta}_V + \psi_V\dot{\psi}_V - \frac{v_{V3}^2\mu_V\left(v_{V3}\right)}{\psi_V^2 + \left\|v_{V3}\right\|^2} \\ = & -\sum_{i=1}^{2}\left(k_{Vi} - \frac{1}{2}\right)\nu_{Vi}^2 - \sum_{i=1}^{2}\left(\lambda_{Vi} - 1\right)\rho_{Vi}^2 + \frac{1}{2}\tilde{\delta}_{V1}^2 + \frac{1}{2}\tilde{\delta}_{V2}^2 \\ & - k_{V3}\nu_{V3}^2 + \nu_{V3}\rho_{V3} - \lambda_{V3}\rho_{V3}^2 + \rho_{V3}\dot{\Delta}x_{V3} + k_{V4}\nu_{V3}\eta_V + \nu_{V3}\Delta u_V \\ & + \eta_V\dot{\eta}_V + \psi_V\dot{\psi}_V - \frac{v_{V3}^2\mu_V\left(v_{V3}\right)}{\psi_V^2 + \left\|v_{V3}\right\|^2} \end{aligned} \tag{41}$$

By using Young's inequality

$$\nu_{V3}\rho_{V3} \leq \frac{1}{2}v_{V3}^2 + \frac{1}{2}\rho_{V3}^2, \quad \dot{\Delta}_{V3}\rho_{V3} \leq \frac{1}{2}\dot{\Delta}_{V3}^2 + \frac{1}{2}\rho_{V3}^2 \tag{42}$$

Substituting (42) into (41), we have

$$\begin{aligned}\dot{V}_{V3} \leq & -\sum_{i=1}^{2}\left(k_{Vi}-\frac{1}{2}\right)\nu_{Vi}^{2}-\sum_{i=1}^{2}\left(\lambda_{Vi}-1\right)\rho_{Vi}^{2}-\left(k_{V3}-\frac{1}{2}\right)\nu_{V3}^{2} \\ & -\left(\lambda_{V3}-1\right)\rho_{V3}^{2}+k_{V4}\nu_{V3}\eta_{V}+\nu_{V3}\Delta u_{V}+\eta_{V}\dot{\eta}_{V}+\psi_{V}\dot{\psi}_{V} \\ & +\frac{1}{2}\tilde{\delta}_{V1}^{2}+\frac{1}{2}\tilde{\delta}_{V2}^{2}+\frac{1}{2}\tilde{\delta}_{V3}^{2}-\frac{v_{V3}^{2}\mu_{V}\left(v_{V3}\right)}{\psi_{V}^{2}+\left\|v_{V3}\right\|^{2}} \\ = & -\sum_{i=1}^{3}\left(k_{Vi}-\frac{1}{2}\right)\nu_{Vi}^{2}-\sum_{i=1}^{3}\left(\lambda_{Vi}-1\right)\rho_{Vi}^{2}+k_{V4}\nu_{V3}\eta_{V}+\nu_{V3}\Delta u_{V} \\ & +\eta_{V}\dot{\eta}_{V}+\psi_{V}\dot{\psi}_{V}+\frac{1}{2}\tilde{\delta}_{V1}^{2}+\frac{1}{2}\tilde{\delta}_{V2}^{2}+\frac{1}{2}\tilde{\delta}_{V3}^{2}-\frac{v_{V3}^{2}\mu_{V}\left(v_{V3}\right)}{\psi_{V}^{2}+\left\|v_{V3}\right\|^{2}}\end{aligned} \tag{43}$$

Applying (34) and (37) into (43) can be written as

$$\begin{aligned}\dot{V}_{V3}= & -\sum_{i=1}^{3}\left(k_{Vi}-\frac{1}{2}\right)\nu_{Vi}^{2}-\sum_{i=1}^{3}\left(\lambda_{Vi}-1\right)\rho_{Vi}^{2}-k_{V\eta}\eta_{V}^{2}-k_{V\psi}\psi_{V}^{2}+\nu_{V3}\Delta u_{V} \\ & +k_{V4}\nu_{V3}\eta_{V}-\left|\nu_{V3}\Delta u_{V}\right|-\frac{1}{2}\Delta u_{V}^{2}-\eta_{V}\Delta u_{V}-\frac{v_{V3}^{2}\mu_{V}\left(v_{V3}\right)}{\psi_{V}^{2}+\left\|v_{V3}\right\|^{2}}-\frac{\mu_{V}\left(v_{3}\right)\psi_{V}^{2}}{\psi_{V}^{2}+\left\|v_{V3}\right\|^{2}} \\ & +\frac{1}{2}\tilde{\delta}_{V1}^{2}+\frac{1}{2}\tilde{\delta}_{V2}^{2}+\frac{1}{2}\tilde{\delta}_{V3}^{2}-k_{V\gamma}\nu_{V3}\mathrm{sig}^{\gamma}\left(\nu_{V3}\right)\end{aligned} \tag{44}$$

As

$$\begin{cases}-\dfrac{v_{V3}^{2}\mu_{V}\left(v_{V3}\right)}{\psi_{V}^{2}+\left\|v_{V3}\right\|^{2}}=-\mu_{V}\left(v_{V3}\right)+\dfrac{\mu_{V}\left(v_{V3}\right)\psi_{V}^{2}}{\psi_{V}^{2}+\left\|v_{V3}\right\|^{2}} \\ \mu_{V}\left(v_{V3}\right)=0.5k_{V4}^{2}v_{V3}^{2},\ \nu_{V3}\Delta u_{V}-\left|\nu_{V3}\Delta u_{V}\right|\leq 0 \\ k_{V4}\nu_{V3}\eta_{V}-\eta_{V}\Delta u_{V}\leq\dfrac{1}{2}k_{V4}^{2}\nu_{V3}^{2}+\eta_{V}^{2}+\dfrac{1}{2}\Delta u_{V}^{2}\end{cases} \tag{45}$$

According to (45), then (43) can be further simplified as

$$\begin{aligned}\dot{V}_{V3} \leq & -\sum_{i=1}^{3}\left(k_{Vi}-\frac{1}{2}\right)\nu_{Vi}^{2}-\sum_{i=1}^{3}\left(\lambda_{Vi}-1\right)\rho_{Vi}^{2}-\left(k_{V\eta}-1\right)\eta_{V}^{2}-k_{V\psi}\psi_{V}^{2} \\ & +\sum_{i=1}^{3}\frac{1}{2}\tilde{\delta}_{Vi}^{2}-k_{V\gamma}\nu_{V3}\mathrm{sig}^{\gamma}\left(\nu_{V3}\right) \\ \leq & -\sum_{i=1}^{3}\left(k_{Vi}-\frac{1}{2}\right)\nu_{Vi}^{2}-\sum_{i=1}^{3}\left(\lambda_{Vi}-1\right)\rho_{Vi}^{2}-\left(k_{V\eta}-1\right)\eta_{V}^{2} \\ & -k_{V\psi}\psi_{V}^{2}+\sum_{i=1}^{3}\frac{1}{2}\tilde{\delta}_{Vi}^{2} \\ \leq & -2\varepsilon_{1}V_{3}+C_{1}\end{aligned} \tag{46}$$

where $\varepsilon_{1}=\min_{1\leq i\leq 3}\left\{\left(k_{Vi}-\frac{1}{2}\right),\left(\lambda_{Vi}-1\right),\left(k_{V\eta}-1\right),k_{V\psi}\right\}$, $C_{1}=\sum_{i=1}^{3}\frac{1}{2}\tilde{\delta}_{Vi}^{2}$, $k_{V\eta}>1$.

If $V_{V3}=P_{1}$, then $\dot{V}_{V3}\leq-\varepsilon P_{1}+C_{1}$. If $\varepsilon_{1}>\frac{C_{1}}{2P_{1}}$, then $V_{V3}=P_{1}$ and $\dot{V}_{V3}\leq 0$. Therefore, $V_{V3}\leq P_{1}$ is an invariant set. In other words, if $V_{V3}\left(0\right)\leq P_{1}$, then $V_{V3}\leq P_{1}$.

Integrate (46) and we can obtain

$$0 \le V_{V3}(t) \le \frac{C_1}{2\varepsilon_1} + \left(V_{V3}(0) - \frac{C_1}{2\varepsilon_1}\right)\exp\left(-2\varepsilon_1 t\right), \quad \forall t \ge 0 \tag{47}$$

Based on the above (47), the bound of $V_3(t)$ is $C_1/(2\varepsilon_1)$. For any $t \ge 0$, $0 \le V_{V3}(t) \le C_1/(2\varepsilon_1)$. Therefore, v_{Vi} $(i = 1, 2, 3)$, ρ_{Vi} $(i = 1, 2, 3)$, η_V and ψ_V are uniformly ultimately bounded.

Therefore, conclusion (i) is proved

According to (47), one can conclude that the $\nu_{Vi} = z_{Vi} - \xi_{Vi}$ $(i = 1, 2, 3)$ is satisfied following

$$|\nu_{Vi}| \le \sqrt{\frac{C_1}{\varepsilon_1}\left(2V_{V3}(0) - \frac{C_1}{\varepsilon_1}\right)\exp\left(-2\varepsilon_1 t\right)} \tag{48}$$

Then

$$\lim_{t\to\infty} |\nu_{Vi}| \le \sqrt{C_1/\varepsilon_1} \tag{49}$$

From (49), we can conclude that ν_{Vi} converges to compact set $R_{v_i} = \left\{\nu_{Vi} \middle| |\nu_{Vi}| \le \sqrt{C_1/\varepsilon_1}\right\}$. That is to say, when ε_1 is chosen large enough, ν_{Vi} converges to any small neighborhood.

From Lemma 2.1, we can get that ξ_{Vi} is bounded. According to $\nu_{Vi} = z_{Vi} - \xi_{Vi}$, further analysis, the velocity tracking error z_{Vi} also converges to any small neighborhood.

Therefore, conclusion (ii) is proved. Theorem 3.1 is proved.

Remark 3.2. *In controller (36), we introduce $k_{V4}\eta_V$ to handle the input saturation of velocity subsystem, mainly for the following two conditions.*

When $\|\eta_V\| \ge \sigma_V > 0$, there is an input saturation in control system.

(a) When $u_{Vc} \ge u_{V\max}$, $k_{V4}\eta_V$ can guarantee that u_{Vc} can reduce to $u_{Vc} = u_{V\max}$.

(b) When $u_{Vc} \le u_{V\min}$, $k_{V4}\eta_V$ can guarantee that u_{Vc} can increase to $u_{Vc} = u_{V\min}$.

Thus, $u_{Vc} = u_{V\max}$ or $u_{Vc} = u_{V\min}$.

When $\|\eta_V\| < \sigma_V$, $\dot{\eta}_V = 0$, there is no input saturation in control system, that is to say $\Delta u_V = 0$, the $k_{V4}\eta_V$ can guarantee that u_{Vc} satisfies $u_{V\min} < u_{Vc} < u_{V\max}$. Thus, $u_V = u_{Vc}$.

3.2. **Adaptive integral terminal sliding mode controller design.** For System (6), refer to the method of velocity subsystem design. Specific process is as follows.

Define the tracking error of the altitude as the following

$$\begin{aligned} z_{1h} &= x_{h1} - x_{hd} \\ z_{2h} &= x_{h2} - x_{h2d} \\ z_{3h} &= x_{h3} - x_{h3d} \\ z_{4h} &= x_{h4} - x_{h4d} \end{aligned} \tag{50}$$

where x_{hd} is altitude reference signal, x_{hjd} $(j = 2, 3, 4)$ the output of the first-order filter with virtual control functions $\bar{x}_{hj}$ $(j = 2, 3, 4)$ as the input.

Define the virtual control functions as

$$\begin{cases} \bar{x}_{h2} = -k_{h1}z_{h1} + \dot{x}_{hd} + \omega_{h1} \\ \bar{x}_{h3} = -k_{h2}z_{h2} - z_{h1} + \dot{x}_{h2d} + \omega_{h2} \\ \bar{x}_{h4} = -k_{h3}z_{h3} - z_{h2} + \dot{x}_{h3d} + \omega_{h3} \end{cases} \tag{51}$$

where k_{h1}, k_{h2} and k_{h3} are positive constants.

Define the first-order filter as

$$\begin{cases} \tau_2\dot{x}_{h2d} + x_{h2d} = \bar{x}_{h2},\ x_{h2d}(0) = \bar{x}_{h2}(0) \\ \tau_3\dot{x}_{h3d} + x_{h3d} = \bar{x}_{h3},\ x_{h3d}(0) = \bar{x}_{h3}(0) \\ \tau_4\dot{x}_{h4d} + x_{h4d} = \bar{x}_{h4},\ x_{h4d}(0) = \bar{x}_{h4}(0) \end{cases} \tag{52}$$

The compensation signal ω_{hj} $(j = 1, 2, 3, 4)$ is constructed by a low-pass filter as

$$\omega_{hj} = -F_{hj}(s)\Delta x_{hj}\ (j = 1, 2, 3, 4) \tag{53}$$

where $F_{hj}(s) = \lambda_{hj}/(s + \lambda_{hj})$ is a low-pass filter.

To eliminate the effect of the errors $x_{hjd} - \bar{x}_{hj}$ $(j = 2, 3, 4)$ caused by the first-order filter, we will design the compensating signals. The compensating signals are defined as

$$\begin{cases} \dot{\xi}_{h1} = -k_{h1}\xi_{h1} + \xi_{h2} + (x_{h2d} - \bar{x}_{h2}) \\ \dot{\xi}_{h2} = -k_{h2}\xi_{h2} - \xi_{h1} + \xi_{h3} + (x_{h3d} - \bar{x}_{h3}) \\ \dot{\xi}_{h3} = -k_{h3}\xi_{h3} - \xi_{h2} + \xi_{h4} + (x_{h4d} - \bar{x}_{h4}) \\ \dot{\xi}_4 = -k_{h4}\xi_{h4} - \xi_{h3} \end{cases} \tag{54}$$

where k_{h4} is a positive constant.

To deal with input saturation problem, the auxiliary system (55) is built up as the following

$$\dot{\eta}_h = \begin{cases} -k_{h\eta}\eta_h - \dfrac{1}{\|\eta_h\|^2}\left(|\nu_{h4}\Delta u_h| + 0.5\Delta u_h^2\right)\eta_h - \Delta u_h - k_{hr}\mathrm{sig}^r(\nu_{h4}), & \|\eta_h\| \geq \sigma_h \\ 0, & \|\eta_h\| < \sigma_h \end{cases} \tag{55}$$

where $\mathrm{sig}^r(\nu_{h4}) = |\nu_{h4}|^r \mathrm{sign}(\nu_{h4})$. $k_{h\eta}$, k_{hr} and r are positive parameters and η_h is the state variable of the auxiliary system. σ_h is a positive constant, $\Delta u_h = u_h - u_{hc}$.

Then, the controller u_{hc} is designed as

$$u_{hc} = -k_{h4}z_{h4} - f_h - z_{h3} + \dot{x}_{h4d} + \omega_4 + k_{h5}\eta_h - \frac{v_{h4}\mu_h(v_{h4})}{\psi_h^2 + \|v_{h4}\|^2} \tag{56}$$

$$\dot{\psi}_h = \begin{cases} -k_{h\psi}\psi_h - \dfrac{\mu_h(v_{h4})\psi_h}{\psi_h^2 + \|v_{h4}\|^2}, & \|v_{h4}\| \geq \psi_{h\nu} \\ 0, & \|v_{h4}\| < \psi_{h\nu} \end{cases} \tag{57}$$

where $\mu_h(v_{h4}) = 0.5k_{h5}^2 v_{h4}^2$, k_{h4}, k_{h5}, $k_{h\psi}$ and $\psi_{h\nu}$ are positive constants.

Theorem 3.2. *Considering system (6) with Assumption 2.2, the state of closed-loop system is regulated under the anti-saturation robust dynamic surface controllers (55)-(57). We can draw the following conclusions.*

(i) The variable v_{hj} $(j = 1, 2, 3, 4)$, η_h, ψ_h are uniformly ultimately bounded;

(ii) The altitude tracking error converges to any small neighborhood.

Proof: The compensated tracking error signal $\nu_{hj} = z_{hj} - \xi_{hj}$ $(j = 1, 2, 3, 4)$ and the compensation error signal $\rho_{hj} = \omega_{hj} + \Delta x_{hj}$ $(j = 1, 2, 3, 4)$.

Consider the Lyapunov function as

$$V_{h4} = \sum_{j=1}^{4}\frac{1}{2}\nu_{hj}^2 + \sum_{j=1}^{4}\frac{1}{2}\rho_{hj}^2 + \frac{1}{2}\eta_h^2 + \frac{1}{2}\psi_h^2 \tag{58}$$

Computing the first order derivative of (58), we obtain

$$\begin{aligned}\dot{V}_{h4} &= \nu_{h1}\dot{\nu}_{h1} + \nu_{h2}\dot{\nu}_{h2} + \nu_{h3}\dot{\nu}_{h3} + \nu_{h4}\dot{\nu}_{h4} + \sum_{j=1}^{4}\rho_{hj}\dot{\rho}_{hj} + \eta_h\dot{\eta}_h + \psi_h\dot{\psi}_h \\ &= -\sum_{j=1}^{3}\left(k_{hj} - \frac{1}{2}\right)\nu_{hj}^2 - \sum_{j=1}^{3}\left(\lambda_{hj} - 1\right)\rho_{hj}^2 + \sum_{j=1}^{3}\sigma_{hj}^2 \\ &\quad + \nu_{h4}\left(\nu_{h3} - k_{h4}z_{h4} + k_{h5}\eta_h - z_{h3} - \dot{\xi}_3\right) \\ &\quad + \nu_{h4}\Delta u_h - \lambda_{h4}\rho_{h4}^2 + \nu_{h4}\rho_{h4} + \dot{\Delta}x_{h4}\rho_{h4} + \eta_h\dot{\eta}_h + \psi_h\dot{\psi}_h - \frac{v_{h4}^2\mu_h\left(v_{h4}\right)}{\psi_h^2 + \left\|v_{h4}\right\|^2}\end{aligned} \tag{59}$$

By using Young's inequality

$$\nu_{h4}\rho_{h4} \le \frac{1}{2}v_{h4}^2 + \frac{1}{2}\rho_{h4}^2, \quad \dot{\Delta}_{h4}\rho_{h4} \le \frac{1}{2}\dot{\Delta}_{h4}^2 + \frac{1}{2}\rho_{h4}^2 \tag{60}$$

Substituting (60) into (59), we have

$$\begin{aligned}\dot{V}_{h4} \le & -\sum_{j=1}^{3}\left(k_{hj} - \frac{1}{2}\right)\nu_{hj}^2 - \sum_{j=1}^{3}\left(\lambda_{hj} - 1\right)\rho_{hj}^2 + \sum_{j=1}^{3}\sigma_{hj}^2 - \left(k_{h4} - \frac{1}{2}\right)\nu_{h4}^2 \\ & - \left(\lambda_{h4} - 1\right)\rho_{h4}^2 + k_{h5}\nu_{h4}\eta_h + \nu_{h4}\Delta u_h + \eta_h\dot{\eta}_h + \psi_h\dot{\psi}_h + \frac{1}{2}\sigma_{h4}^2 - \frac{v_{h4}^2\mu_h\left(\nu_{h4}\right)}{\psi_h^2 + \left\|\nu_{h4}\right\|^2} \\ = & -\sum_{j=1}^{4}\left(k_{hj} - \frac{1}{2}\right)\nu_{hj}^2 - \sum_{j=1}^{4}\left(\lambda_{hj} - 1\right)\rho_{hj}^2 + \sum_{j=1}^{4}\sigma_{hj}^2 + k_{h5}\nu_{h4}\eta_h \\ & + \nu_{h4}\Delta u_h + \eta_h\dot{\eta}_h + \psi_h\dot{\psi}_h - \frac{v_{h4}^2\mu_h\left(\nu_{h4}\right)}{\psi_h^2 + \left\|\nu_{h4}\right\|^2}\end{aligned} \tag{61}$$

Substituting (55) and (57) into (61), we obtain

$$\begin{aligned}\dot{V}_{h4} = & -\sum_{j=1}^{4}\left(k_{hj} - \frac{1}{2}\right)\nu_{hj}^2 - \sum_{j=1}^{4}\left(\lambda_{hj} - 1\right)\rho_{hj}^2 - k_{h\eta}\eta_h^2 - k_{h\psi}\psi_h^2 + k_{h5}\nu_{h4}\eta_h \\ & + \nu_{h4}\Delta u_h - \left|\nu_{h4}\Delta u_h\right| - \frac{1}{2}\Delta u_h^2 - \eta_h\Delta u_h - \frac{v_{h4}^2\mu_h\left(\nu_{h4}\right)}{\psi_h^2 + \left\|\nu_{h4}\right\|^2} - \frac{\mu_h\left(\nu_{h4}\right)\psi_h^2}{\psi_h^2 + \left\|\nu_{h4}\right\|^2} \\ & + \sum_{j=1}^{4}\sigma_{hj}^2 - k_{hr}\nu_{h4}\mathrm{sig}^r\left(\nu_{h4}\right)\end{aligned} \tag{62}$$

As

$$\begin{cases} -\dfrac{v_{h4}^2\mu_h\left(\nu_{h4}\right)}{\psi_h^2 + \left\|\nu_{h4}\right\|^2} = -\mu_h\left(v_{h4}\right) + \dfrac{\mu_h\left(\nu_{h4}\right)\psi_h^2}{\psi_h^2 + \left\|\nu_{h4}\right\|^2} \\ \mu_h\left(v_{h4}\right) = 0.5k_{h5}^2v_{h4}^2, \quad \nu_{h4}\Delta u_h - \left|\nu_{h4}\Delta u_h\right| \le 0 \\ k_{h5}\nu_{h4}\eta_h - \eta_h\Delta u_h \le \dfrac{1}{2}k_{h5}^2v_{h4}^2 + \eta_h^2 + \dfrac{1}{2}\Delta u_h^2 \end{cases} \tag{63}$$

according to (63), then (62) can be further simplified as

$$\begin{aligned}\dot{V}_{h4} \leq & -\sum_{j=1}^{4}\left(k_{hj}-\frac{1}{2}\right)\nu_{hj}^2-\sum_{j=1}^{4}\left(\lambda_{hj}-1\right)\rho_{hj}^2-\left(k_{h\eta}-1\right)\eta_h^2-k_{h\psi}\psi_h^2 \\ & +\sum_{j=1}^{4}\sigma_{hj}^2-k_{hr}\nu_{h4}\mathrm{sig}^r\left(\nu_{h4}\right) \\ \leq & -\sum_{j=1}^{4}\left(k_{hj}-\frac{1}{2}\right)\nu_{hj}^2-\sum_{j=1}^{4}\left(\lambda_{hj}-1\right)\rho_{hj}^2-\left(k_{h\eta}-1\right)\eta_h^2-k_{h\psi}\psi_h^2+\sum_{j=1}^{4}\sigma_{hj}^2 \\ \leq & -2\varepsilon_2 V_{h4}+C_2\end{aligned} \tag{64}$$

where $\varepsilon_2=\min_{1\leq j\leq 4}\left\{\left(k_{hj}-\frac{1}{2}\right),\left(\lambda_{Vj}-1\right),\left(k_{V\eta}-1\right),k_{V\psi}\right\}$, $C_2=\sum_{i=1}^{4}\sigma_{hi}^2$, $k_{h\eta}>1$.

Similar to Theorem 3.1, one can conclude that the $\nu_{hj}=z_{hj}-\xi_{hj}$ $(j=1,2,3,4)$ is satisfied following

$$|\nu_{hj}|\leq\sqrt{\frac{C_2}{\varepsilon_2}\left(2V_{h4}(0)-\frac{C_2}{\varepsilon_2}\right)\exp\left(-2\varepsilon_2 t\right)} \tag{65}$$

Then

$$\lim_{t\to\infty}|\nu_{hj}|\leq\sqrt{C_2/\varepsilon_2} \tag{66}$$

From (66), we can conclude that ν_{hj} converges to compact set $R_{h_j}=\left\{\nu_{hj}\middle||\nu_{hj}|\leq\sqrt{C_2/\varepsilon_2}\right\}$, that is to say, when ε_2 is chosen large enough, ν_{hj} converges to any small neighborhood.

From Lemma 2.1, we can get that the ξ_{hj} is bounded. According to $\nu_{hj}=z_{hj}-\xi_{hj}$, further analysis, the velocity tracking error z_{hj} also converges to any small neighborhood.

Therefore, conclusion (ii) is proved

Therefore, Theorem 3.2 is proved.

Remark 3.3. *In controller (56), we introduce $k_{h5}\eta_h$ to handle the input saturation of velocity subsystem, mainly for the following two conditions.*

When $\|\eta_h\|\geq\sigma_h>0$, there is input saturation in control system.

(a) When $u_{hc}\geq u_{h\max}$, $k_{h5}\eta_h$ can guarantee that u_{hc} can reduce to $u_{hc}=u_{h\max}$.

(b) When $u_{hc}<u_{h\max}$, $k_{h5}\eta_h$ can guarantee that u_{hc} can increase to $u_{hc}=u_{h\min}$.

Thus, $u_{hc}=u_{h\max}$ or $u_{hc}=u_{h\min}$.

When $\|\eta_h\|<\sigma_h$, $\dot{\eta}_h=0$, there is no input saturation in control system, that is to say $\Delta u_h=0$. $k_{h5}\eta_h$ can guarantee that u_{hc} satisfies $u_{h\min}<u_{hc}<u_{h\max}$. Thus $u_h=u_{hc}$.

4. **Numerical Examples.** In order to verify the effectiveness of the two robust backstepping controllers, we take the nonlinear longitudinal motion (1) of the hypersonic vehicles in this chapter as the simulation object. The parameters of the hypersonic vehicles and flight environment of [10] are shown in Table 1 and the values of the aerodynamic coefficients are shown in Table 2.

Based on the basic parameters of the above hypersonic vehicles, we can figure out a group of equilibrium points as the initial condition, and the initial value of simulation is set as $\boldsymbol{x}(0)=[4590.3\ \ 33528\ \ 0.0334\ \ 0.0334\ \ 0\ \ 0.1802\ \ 0]^T$. In the simulation process, the external disturbances $d_1(t)=0.0024\sin(0.2t)$, $d_2(t)=0.012\sin(0.2t)$. The parameter

TABLE 1. The parameters of hypersonic aircrafts and flight environment

Physical quantity	Symbol	Value
Mass (kg)	m	1.378×10^5
Moment of inertia (kg m^2)	I_{yy}	9.5×10^6
Reference area (m^2)	S	335.2
Mean aerodynamic chord (m)	$\bar{c}$	24.384
Earth radius (m)	R_E	6.371004×10^6
Gravitational constant (N m/kg^2)	μ	3.9802×10^{14}
Altitude (m)	h	33528
Velocity (m/s)	V	4590.288
Atmospheric density (kg/m^3)	ρ	0.0125368

TABLE 2. The values of the aerodynamic coefficients

Coefficient	Value	Coefficient	Value	Coefficient	Value
C_L^{α}	0.6203	$C_{M,\alpha}^{\alpha}$	0.036617	β_0'	0.00336
$C_D^{\alpha^2}$	0.6450	$C_{M,\alpha}^{0}$	5.3261×10^{-6}	β_1	0.0224
C_D^{α}	0.0043378	C_M^0	0.0292	$C_{M,\alpha}^{\alpha^2}$	-0.035
C_D^0	0.003772	$C_{M,q}^{\alpha^2}$	-6.796	$C_{M,q}^0$	-0.2289
β_0	0.02576	$C_{M,q}^{\alpha}$	0.3015	c_e	-12897

uncertainties of the model are selected

$$\begin{aligned} &m = m_0\,(1+\Delta m)\,,\ I_{yy} = I_0\,(1+\Delta I_{yy}) \\ &S = S_0\,(1+\Delta S)\,,\ c = c_0\,(1+\Delta c) \\ &c_e = c_{e0}\,(1+\Delta c_{e0})\,,\ \rho = \rho_0\,(1+\Delta\rho) \\ &|\Delta m| \le 0.05,\ |\Delta I_{yy}| \le 0.05,\ |\Delta S| \le 0.05 \\ &|\Delta c| \le 0.05,\ |\Delta\rho| \le 0.05,\ |\Delta c_e| \le 0.05 \end{aligned} \tag{67}$$

where m_0, I_0, S_0, c_0, c_{e0}, ρ_0 are normal values respectively, the parameter uncertainties of the model are set as $\Delta m = -0.05$, $\Delta I_{yy} = -0.05$, $\Delta c = 0.05$, $\Delta c_e = 0.05$, $\Delta\rho = 0.05$, $\Delta S = 0.05$.

4.1. **Simulation analysis of the robust dynamic surface controller considering the control saturation.** To verify the validity of the control strategy of the hypersonic vehicles designed in this paper, we have added a comparison with second-order terminal sliding mode control (2TSMTC) [33]. The simulations select two kinds of reference signals as tracking signals. The control gains and parameters are shown in Table 3.

Situation 1: The reference velocity of the hypersonic vehicles is $V_d = 4690.3$ m/s, that is, $\Delta V = 100$ m/s, and the reference altitude is $h_d = 35028$ m, that is, $\Delta h = 1500$ m.

Situation 2: The reference velocity of the hypersonic vehicles is $V_d = 4670.3$ m/s, that is, $\Delta V = (100 + t)$ m/s, and the reference altitude is $h_d = 35028$ m, that is, $\Delta h = (1500 + t^2)$ m.

(1) For the situation 1, the simulation results are shown in Figures 1-4.

Figure 1 and Figure 2 show the tracking curves of velocity and altitude of hypersonic vehicles, respectively. From Figures 1 and 2, it can be seen that even if there are mismatched uncertainties and input saturation, the velocity error and altitude error can converge rapidly, satisfying the requirement of control accuracy. Figure 3 illustrates the

TABLE 3. The set of the parameters of controllers

Parameter	Value	Parameter	Value	Parameter	Value	Parameter	Value
k_{V1}	15	ψ_V	0.01	$k_{V\eta}$	3.5	λ_{V2}	0.1
k_{V2}	25	τ_{V2}	0.01	$k_{V\gamma}$	1.5	γ	0.75
k_{V3}	12	τ_{V3}	0.01	$k_{V\psi}$	0.8	λ_{V3}	0.1
k_{V4}	0.3	λ_{V1}	0.1	σ_V	0.01	τ_{V3}	0.01
k_{h1}	15	τ_{h2}	0.01	$k_{h\eta}$	2.5	λ_{h3}	0.1
k_{h2}	8	τ_{h3}	0.01	$k_{h\psi}$	0.65	λ_{h4}	0.1
k_{h3}	3.2	τ_{h4}	0.01	σ_h	0.01	k_{hr}	3.5
k_{h4}	16	λ_{h1}	0.1	ψ_h	0.01	r	0.8
k_{h5}	0.6	λ_{h2}	0.1				

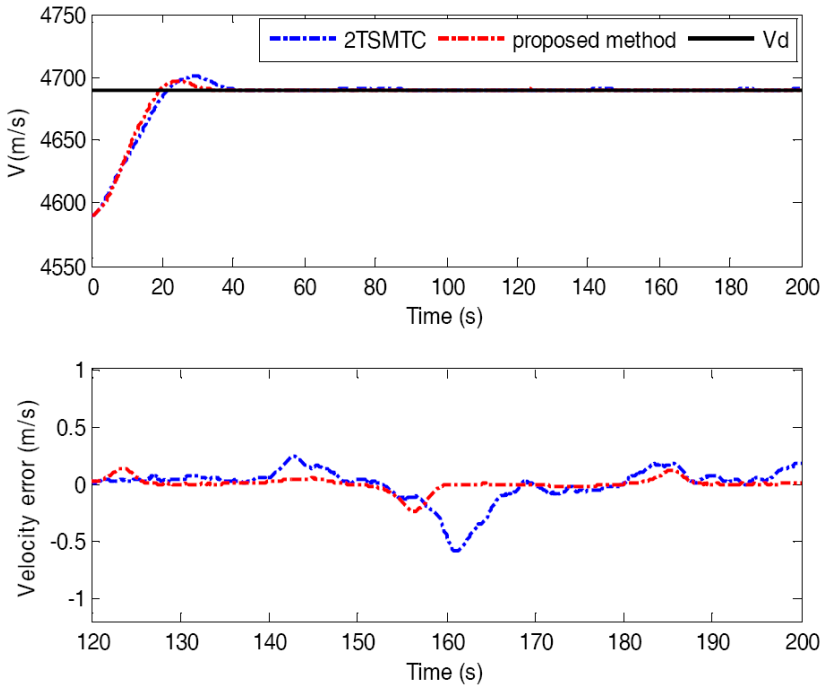

FIGURE 1. The tracking curves of velocity

curves of control input, suggesting that the amplitude of the control force accords with the control constraint. As the simulation results show, the control input signals ϕ_c and δ_e are continuous and smooth which make the proposed control laws possible for the actual flight implementation. The curves of the attack angle, the pitch angle and the pitch rate depicted in Figure 4, are quite smooth and within their rational bounds.

(2) For the situation 2, its control parameters and gains and reference signal are the same as those of the situation 1 and the simulation results are shown in Figures 5-8.

From Figures 5-8, when the reference signals are time-varying signals, for the longitudinal model of the hypersonic vehicle, both the velocity and altitude can track their reference signals under proposed control strategy. So this part will focus on the analysis of the differences between the two situations. From Figures 5 and 6, it can be obtained that the proposed method and 2TSMTC can achieve the stable tracking of the velocity V and altitude h of the reference command. The curves of control inputs under the proposed method and 2TSMTC are shown in Figure 7. It can be obtained that the curve of the control input ϕ_c and δ_e under the proposed method are smooth and can converge to

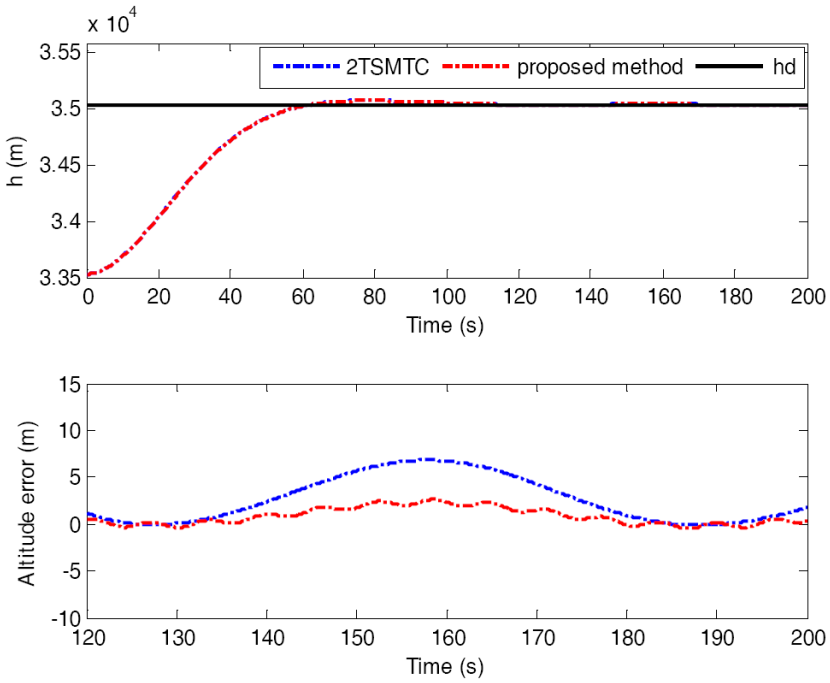

FIGURE 2. The tracking curves of altitude

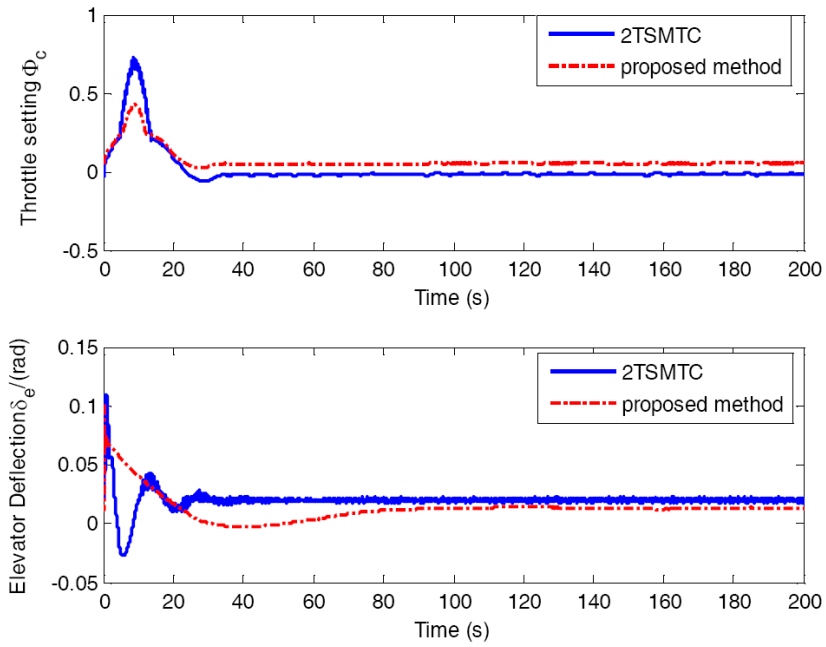

FIGURE 3. The curves of the control inputs ϕ_c, δ_e

a small neighbourhood of zero in tracking process with a smaller control gain compared with 2TSMTC. From Figure 8, it can be known that the curves of the angle of attack α, the pitch angle θ, and the pitch rate q approach their steady-state values in short time. In summary, simulation results show that the robust DSC control scheme possesses a good adjustment capacity and a strong robustness for the longitudinal model of the hypersonic vehicle with mismatched uncertainties and input saturation, which can guarantee the stability of the system tracking performance.

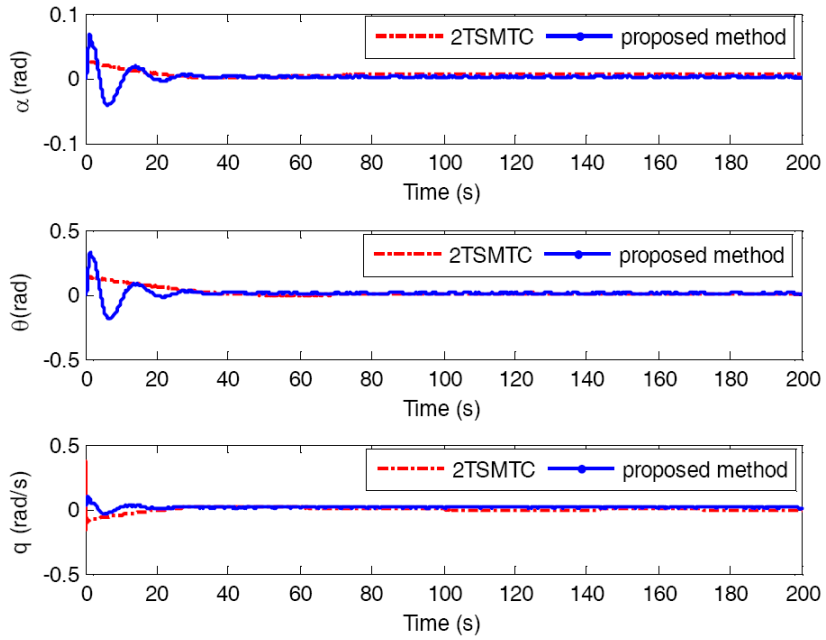

FIGURE 4. The curves of the α, θ and q

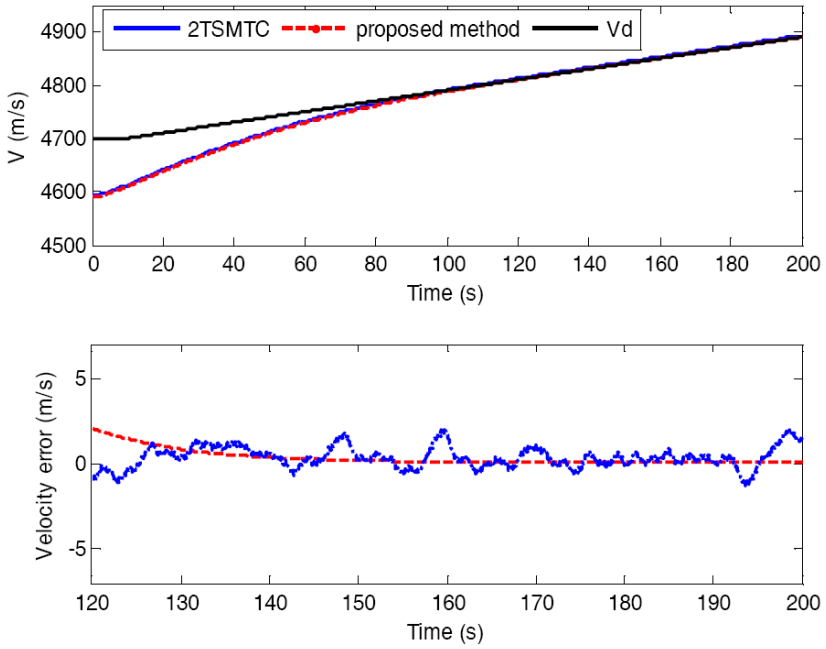

FIGURE 5. The tracking curves of velocity

5. **Conclusions.** This paper studies the saturated tracking performance of hypersonic vehicles on the basis of the DSC with signal compensation and auxiliary system. The conclusions are as the following.

(1) The non linear control system model of hypersonic vehicles is simplified by the input and output linearization, and reasonably decomposed into subsystems that include velocity subsystem and altitude subsystem.

(2) A robust back-stepping control scheme is designed using the DSC with signal compensation method and the auxiliary system, which can eliminate the effect of mismatched uncertainties equivalents thoroughly and handle the impact of input saturation.

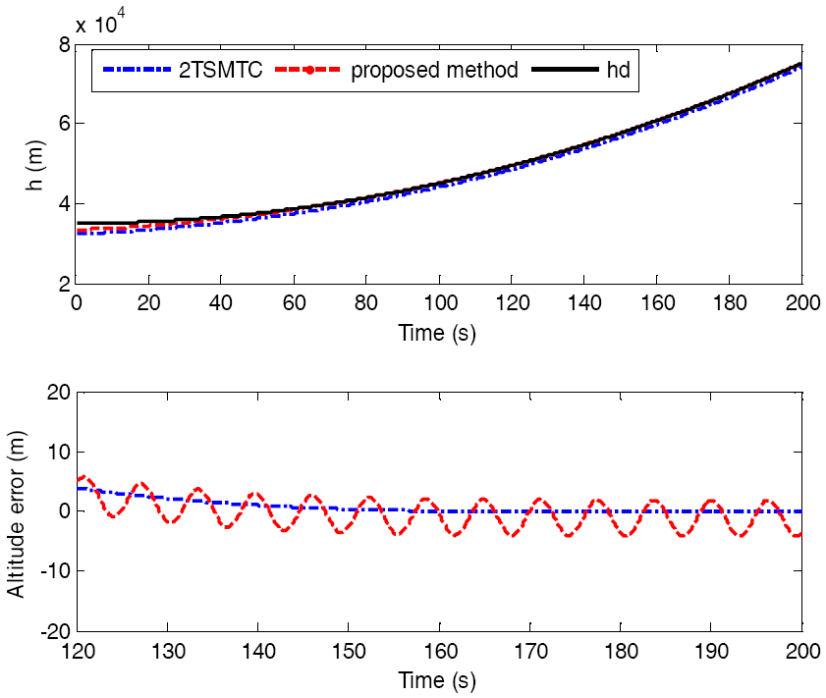

FIGURE 6. The tracking curves of altitude

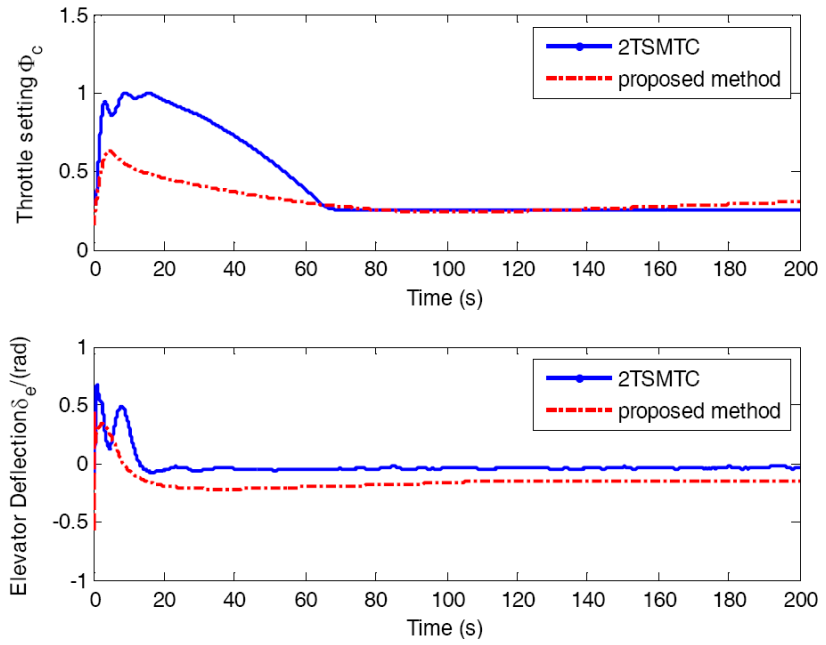

FIGURE 7. The curves of the control inputs ϕ_c, δ_e

(3) The simulation results demonstrate the robustness of controllers for mismatched uncertainties and good tracking performance of the desired reference signals.

(4) In the future, the problem of elasticity and non-minimum phase should be considered in the design hypersonic control system. Based on the existing control algorithm, the different advanced control methods should be combined with each other to improve the performance of the control algorithm and solve the control problem.

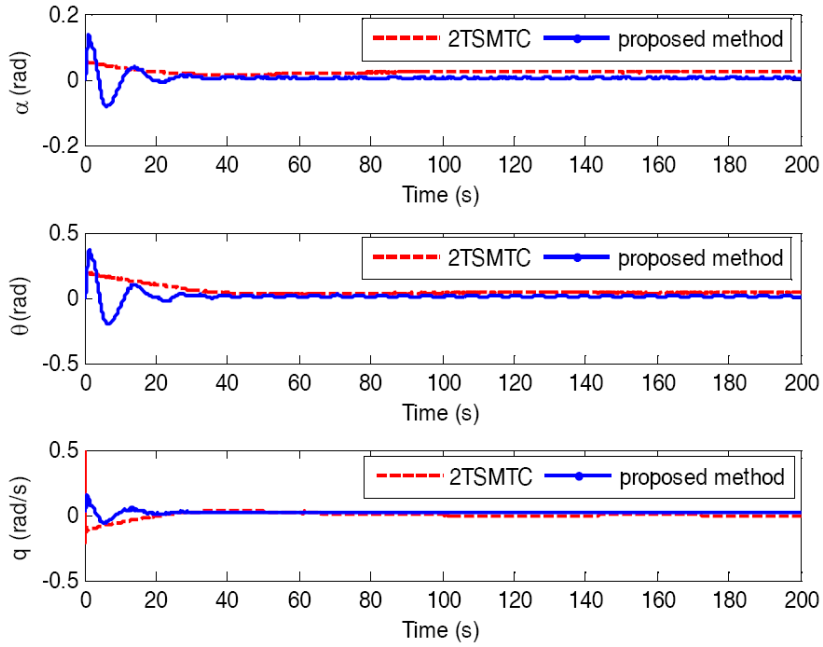

FIGURE 8. The curves of the α, θ and q

Acknowledgment. The authors would like to acknowledge the financial support provided by the Aeronautical Science Foundation of China (20140177002), Foundation for Creative Research Groups of the National Natural Science Foundation (61021002).

REFERENCES

[1] L. Huang, Z. S. Duan and J. Y. Yang, Challenges of control science in near space hypersonic aircrafts, *Control Theory & Applications*, vol.28, no.10, pp.1496-1505, 2011.

[2] B. Xu, D. W. Wang, F. C. Sun and Z. K. Shi, Direct neural discrete control of hypersonic flight vehicle, *Nonlinear Dynamics*, vol.70, no.1, pp.269-278, 2012.

[3] Z. T. Dydek, A. M. Annaswamy and E. Lavretsky, Adaptive control and the NASA X-15-3 flight revisited, *Control Systems*, vol.30, no.3, pp.32-48, 2010.

[4] B. Xu and Z. K. Shi, An overview on flight dynamics and control approaches for hypersonic vehicles, *Science China Information Sciences*, vol.58, no.7, pp.1-19, 2015.

[5] C. Y. Sun, C. X. Mu and Y. Yao, Some control problems for near space hypersonic vehicles, *Acta Automatica Sinica*, vol.39, no.11, pp.1901-1913, 2013.

[6] F. Chavez and D. Schmidt, Uncertainty modeling for multivariable-control robustness analysis of elastic high-speed vehicles, *Journal of Guidance, Control, and Dynamics*, vol.22, no.1, pp.87-95, 1999.

[7] J. Davidson, F. Lallman and J. Mcminn, Flight control laws for NASA's hyper-X research vehicle, *AIAA Guidance, Navigation and Control Conference and Exhibit*, Portland, pp.1-9, 1999.

[8] Q. Wang and R. Stengel, Robust nonlinear control of a hypersonic aircraft, *Journal of Guidance, Control, and Dynamics*, vol.23, no.4, pp.577-585, 2000.

[9] H. Xu, M. D. Mirmirani and P. A. Ioannou, Adaptive sliding mode control design for a hypersonic flight vehicle, *Journal of Guidance, Control, and Dynamics*, vol.27, no.5, pp.829-838, 2004.

[10] H. B. Sun, S. H. Li and C. Y. Sun, Finite time integral sliding mode control of hypersonic vehicles, *Nonlinear Dynamics*, vol.73, nos.1-2, pp.229-244, 2013.

[11] Y. Yi, L. B. Xu, H. Shen and X. X. Fan, Disturbance observer-based L1 robust tracking control for hypersonic vehicles with TS disturbance modeling, *International Journal of Advanced Robotic Systems*, vol.13, no.6, 2016.

[12] H. An, J. X. Liu, C. H. Wang and L. G. Wu, Disturbance observer-based antiwindup control for air-breathing hypersonic vehicles, *IEEE Trans. Industrial Electronics*, vol.63, no.5, pp.3038-3049, 2016.

[13] J. T. Parker, A. Serrani and S. Yurkovich, Control-oriented modeling of an air-breathing hypersonic vehicle, *Journal of Guidance, Control, and Dynamics*, vol.30, no.3, pp.856-869, 2007.
[14] H. Buschek and A. J. Calise, Uncertainty modeling and fixed-order controller design for a hypersonic vehicle model, *Journal of Guidance, Control, and Dynamics*, vol.20, no.1, pp.42-48, 1997.
[15] R. Y. Qi, Y. H. Huang, B. Jiang and G. Tao, Adaptive back-stepping control for a hypersonic vehicle with uncertain parameters and actuator faults, *Proc. of the Institution of Mechanical Engineers, Part I: Journal of Systems and Control Engineering*, vol.227, no.1, pp.51-61, 2013.
[16] Y. L. Li, M. Zeng, H. An and C. H. Wang, Disturbance observer-based control for nonlinear systems subject to mismatched disturbances with application to hypersonic flight vehicles, *International Journal of Advanced Robotic Systems*, vol.14, no.2, 2017.
[17] Y. Y. Zhang, R. F. Li, X. Gao and Z. K. Lei, Exponential sliding mode tracking control via back-stepping approach for a hypersonic vehicle with mismatched uncertainty, *Journal of the Franklin Institute*, vol.353, no.10, pp.2319-2343, 2016.
[18] D. X. Gao, S. X. Wang and H. J. Zhang, Singularly perturbed system approach to adaptive neural back-stepping control design of hypersonic vehicles, *Journal of Intelligent & Robotic Systems*, vol.73, nos.1-4, pp.249-259, 2014.
[19] B. Xu, D. W. Dan, H. Wang and S. Q. Zhu, Adaptive neural control of a hypersonic vehicle in discrete time, *Journal of Intelligent & Robotic Systems*, vol.73, nos.1-4, pp.219-231, 2014.
[20] Y. M. Li and S. C. Tong, Hybrid adaptive fuzzy control for uncertain MIMO nonlinear systems with unknown dead-zones, *Information Sciences*, no.328, pp.97-114, 2016.
[21] W. Dong, J. A. Farrell and M. M. Polycarpou, Command filtered adaptive back-stepping, *IEEE Trans. Control Systems Technology*, vol.20, no.3, pp.566-580, 2012.
[22] J. P. Yu, P. Shi and W. J. Dong, Observer and command-filter-based adaptive fuzzy output feedback control of uncertain nonlinear systems, *IEEE Trans. Industrial Electronics*, vol.62, no.9, pp.5962-5970, 2015.
[23] Y. Cui, H. G. Zhang, Y. C. Wang and Z. Zhang, Adaptive neural dynamic surface control for a class of uncertain nonlinear systems with disturbances, *Neurocomputing*, vol.165, pp.152-158, 2015.
[24] M. Chen, S. Z. S. Ge and B. B. Ren, Adaptive tracking control of uncertain MIMO nonlinear systems with input constraints, *Automatica*, vol.47, no.3, pp.452-465, 2011.
[25] M. Chen, G. Tao and B. Jiang, Dynamic surface control using neural networks for a class of uncertain nonlinear systems with input saturation, *IEEE Trans. Neural Networks and Learning Systems*, vol.26, no.9, pp.2086-2097, 2015.
[26] X. L. Cheng, P. Wang, L. H. Liu and G. J. Tang, Disturbance rejection control for attitude control of air-breathing hypersonic vehicles with actuator dynamics, *Proc. of the Institution of Mechanical Engineers, Part I: Journal of Systems and Control Engineering*, vol.230, no.9, pp.988-1000, 2016.
[27] H. J. Yang, Y. Yu, F. Wang and K. F. Lu, Active disturbance rejection attitude control for a hypersonic reentry vehicle with actuator saturation, *International Journal of Advanced Robotic Systems*, vol.14, no.3, 2017.
[28] F. Wang, Q. Zou, C. C. Hua and Q. Zong, Dynamic surface tracking controller design for a constrained hypersonic vehicle based on disturbance observer, *International Journal of Advanced Robotic Systems*, vol.14, no.3, 2017.
[29] Q. Zong, F. Wang, R. Su and S. K. Shao, Robust adaptive back-stepping tracking control for a flexible air-breathing hypersonic vehicle subject to input constraint, *Proc. of the Institution of Mechanical Engineers, Part G: Journal of Aerospace Engineering*, vol.229, no.1, pp.10-25, 2015.
[30] Q. Zong, F. Wang, B. L. Tian and R. Su, Robust adaptive approximate back-stepping control of a flexible air-breathing hypersonic vehicle with input constraint and uncertainty, *Proc. of the Institution of Mechanical Engineers, Part I: Journal of Systems and Control Engineering*, vol.228, no.7, pp.521-539, 2014.
[31] X. W. Bu, X. Y. Wu, M. Y. Tian, J. Q. Huang and R. Zhang, High-order tracking differentiator based adaptive neural control of a flexible air-breathing hypersonic vehicle subject to actuators constraints, *ISA Transactions*, vol.58, pp.237-247, 2015.
[32] Q. Zong, F. Wang, B. L. Tian and R. Su, Robust adaptive dynamic surface control design for a flexible air-breathing hypersonic vehicle with input constraints and uncertainty, *Nonlinear Dynamics*, vol.78, no.1, pp.289-315, 2014.
[33] R. M. Zhang, C. Y. Sun, J. M. Zhang and Y. J. Zhou, Second-order terminal sliding mode control for hypersonic vehicle in cruising flight with sliding mode disturbance observer, *Journal of Control Theory and Applications*, vol.11, no.2, pp.299-305, 2013.